Ionospheric Response to the Particular Solar Event as Seen in the Ionospheric Vertical Sounding

Z. Mošna,[1,2] P. Šauli,[2] and K. Georgieva[3]

[1] Charles University, Faculty of Mathematics and Physics, Prague, Czech Republic.
[2] Institute of Atmospheric Physics, Academy of Sciences, Prague, Czech Republic.
[3] Solar-Terrestrial Influences Laboratory at the Bulgarian Academy of Sciences, Sofia, Bulgaria.

Abstract. Two types of solar events are mainly responsible for geomagnetic and ionospheric (geospheric) disturbances, (1) Coronal Mass Ejection (CME), including its manifestation as Magnetic Cloud (MC) with rotational magnetic field, and (2) High Speed Solar Stream (HSS) associated with the coronal holes. Each type has a different ability to impact the geosphere. Three solar events in 2004 were selected to study the ionospheric response above the Pruhonice observatory. The Magnetic Cloud with the leftward rotation of magnetic field (MC L) on November 07, 2004 and the HSS event on March 09, 2004 were followed by a significant decrease of the plasma density in the ionospheric height profiles and a sharp ascent of the F2-layer, while the ionospheric response to the Magnetic Cloud with the rightward rotation (MC R) on February 11, 2004 did not show significant changes in the height of F2-layer or the peak plasma density. In all of the studied events, wave-like oscillations of the virtual heights of F2 were observed in response to the impact.

Introduction

The ionosphere is a part of the atmosphere sufficiently ionized to affect the propagation of radio waves. The height profile of the plasma density in the ionosphere can be characterized by means of the vertical ionospheric sounding. Depending on time of day, season, geomagnetic conditions, and other space weather events, the ionosphere splits into several layers of enhanced plasma concentration (*Davies, K.*,[1990]). Since 1958, Pruhonice observatory (50.1N, 14.5E) operates an ionospheric sounder that observes stratification of the ionosphere into the E and F (F1 and F2) layers by means of the vertical HF sounding in which an electromagnetic wave signal is transmitted upward, reflected from the ionosphere, and received on the ground. Typical ionogram from the Pruhonice observatory and a description of derived ionospheric characteristics can be found e.g. in *Mosna et al.*, [2008].

The ionosphere is a highly variable system. It is sensitive to the solar and geomagnetic activity, as well as dynamic events in the neutral atmosphere. Disturbances of the ionospheric plasma affect operation of various communication and navigation systems, e.g. GPS, GALILEO, Glonas (*Belehaki et al.*, [2007]). Miscellaneous models of ionosphere use number of sunspots, geomagnetic indices, day and year time, etc.(*Mikhailov et al.* [1996], *Zolesi et al.* [1993], *Cander, L.*, [2009]) to predict state of the ionosphere. In recent years, response of the ionospheric plasma to the solar events is studied internationally. In 2004, a new digisonde DPS-4 replaced previously operating IPS-KEL Aerospace ionosonde at Pruhonice observatory. The DPS-4 digisonde allows additional measurements of the reflected signal, including its angle of arrival and polarization (*Huang and Reinisch*, [1996], *Reinisch et al.*, [2005]).

In our paper, we investigate response of the ionosphere to various types of solar events that drive active processes in terrestrial plasma. The solar events will be categorized by the magnetic field configuration of the associated coronal structures.

First group of solar events is characterized by poloidal magnetic field. During the solar maximum periods, High Speed Solar Streams are formed in the areas of solar coronal holes that are long lived regions of open magnetic field lines. The solar wind flowing from them has

high speed, low plasma density and high plasma temperature. Second group is characterized by toroidal magnetic field. Coronal Mass Ejections (CMEs) and their subset, Magnetic Clouds (MCs), originate in the regions of closed magnetic field lines rooted at both sides in the Sun. They are examples of short term events. CMEs have low proton temperature (low plasma beta). MCs are distinguished by high magnetic field, smooth rotation of B and decreased plasma temperature *Burlaga et al.*, [1981]. It has been shown that these different types of solar events influence differently the Earth's magnetosphere. A term 'geoeffectiveness' has been introduced to describe this influence (*Georgieva et al.*, [2006], *Richardson et al.*, [2002]). MCs are found to be more geoeffective drivers of the geomagnetic activity by means of DST response than CMEs without rotation of B (*Georgieva and Kirov*, [2005]).

For our study, we have selected one HSS event and two MC types, with the leftward rotation of the magnetic field (MC L) and the right-oriented MC R. The task of our paper is to investigate ionospheric response to onset of each of the events and observe whether contrariwise rotation of the magnetic field affects MCs ability to impact ionospheric characteristics.

Data

We have selected three different types of solar events of 2004, together with appropriate geomagnetic indices DST and ionospheric data. According to the definition of HSS ($v > 500$ km s^{-1} and increase of velocity of more than 100 km s^{-1} within one day, accompanied by high plasma temperature and low plasma density) and MC (high magnetic field, low beta and smooth magnetic field rotation) (*Georgieva et al.*, [2006]), we have chosen the HSS event of March 09, 7 UT; the MC L event of November 07, 6 UT (during a "superstorm"), and the MC R event of February 11, 7 UT. Selected MC L event was followed by another MC L two days later. Measurements of magnetic field, plasma density and solar wind velocity were made by the ACE satellite, publicly available in the NASA CDAWeb database (`http://cdaweb.gsfc.nasa.gov/`). Total magnetic fields B, magnetic components in GSE B_x, B_y, B_z and velocities are shown in Fig. 1. All events are characterized by B_z negative component. The events were chosen to have the most similar properties (B_z negative etc.) as possible. After removing of potential events when ionospheric data were not possible to analyze (e.g. useless inograms with missing traces etc.) we chose HSS and MC R with similar values of B and B_z and MC L with three times larger values of B and B_z.

For each event we manually processed eleven days of ionograms with the regular 15 minute cadence. Four days prior to the event serve as the normal state reference. We study the ionospheric response during remaining days after the event. From ionograms, we derived profilograms (time series of the ionospheric plasma frequency profile), critical frequencies foF2 (maximum plasma frequency of the ionosphere), and virtual heights of bottom of the F2 layer h'F2. The values h'F2 are computed from the time of flight of the reflected electromagnetic signal under assumption that its velocity equals to the velocity of light (*Shapley*, [1970]). Another value, the height of the maximum electron concentration hmF2, is probably as well suitable for the analyse. The advantage of value h'F2 comes from the reason that it is directly measured from the trace on the ionogram while the value hmF2 is derived from the model of ionospheric profile. Difference in results from NHPC and Polan models under disturbed conditions is described in *Sauli et al.*, [2007]. However, we will think about using both values in future work.

In general, geomagnetic disturbances had several hour delay after the beginning of the event as recorded on the satellite (reference time). The transit time of the solar matter with an increased velocity during the event to reach the Earth from the distance of the satellite is less than one hour.

In present paper, we characterize ionospheric plasma by means of the plasma frequencies since the ionosonde records the reflected electromagnetic waves with the frequency which corresponds to the plasma frequency in the ionosphere. A conversion between typical plasma frequencies in E and F layers and the electron concentrations is in Tab. 1.

Table 1. Conversion table between typical ionospheric plasma frequencies and electron concentrations.

Plasma frequency (MHz)	2	4	6	8	10	12
Electron concentration (10^3 cm^{-3})	50	200	440	790	1230	1780

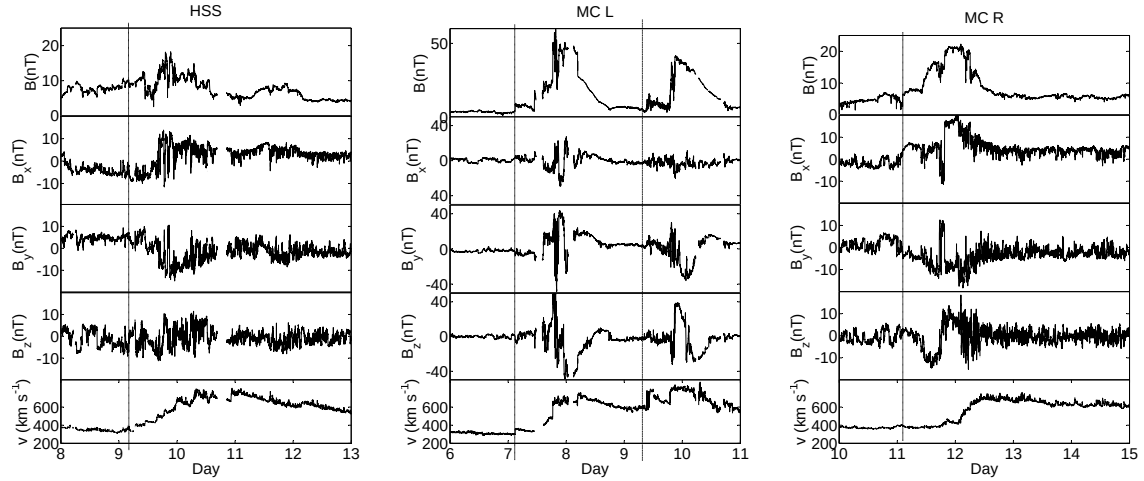

Figure 1. Records of total magnetic field B (upper panels), components Bx, By and Bz (middle), and velocity of solar wind (bottom panels) in GSE during HSS (left), MC L, and MC R (right). Dashed lines denote starts of the events. Dotted line in MC L shows following event two days later.

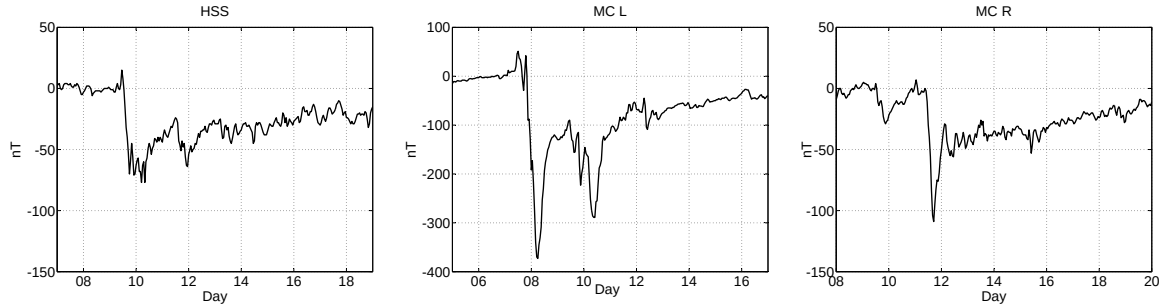

Figure 2. Dst indices in HSS, MCL and MCR (from left). Note different y-scale in MC L. The highest response is in MCR case while the responses to HSS and MCL are comparable.

Fig. 2 presents similar values of Dst for the HSS and MC R events, while the Dst response to MC L is three times stronger which correspond to the B (B_z) of the events.

Results and Discussion

HSS: Bottomside ionospheric density starts decreasing approximately half a day after the morning event, in the evening hours. Both daytime and nighttime foF2 reduce. Night foF2 values are >30 percent below the normal and daytime foF2 are reduced by >10 percent. Virtual heights h'F2 a) increase from 300 km during the daytime to more than 350 km and b) exhibit wavelike oscillations after HSS. The oscillation may indicate passage of the Traveling Ionospheric

Disturbance (TID) moving from the polar to equatorial areas along the magnetic field lines. Plasma densities at all heights of the profile decrease in comparison to the reference days.

MC L: This event is followed by another solar event two days later. We observe three days of strong oscillations and rapid sharp changes of h'F2 as seen in Fig. 4. First ionospheric response is seen in h'F2 within only few hours after MC L measured on the satellite. After the first event daytime foF2 values rapidly drop below 5 MHz on the next day after the event (upper left panel on the Fig. 4). The ionospheric densities recover quickly and we observe return of foF2 to its previous typical values (9 MHz, two days after event). Then, when second event occurs, we observe another drop of foF2 values below 5 MHz (see Fig. 4). During all last seven days after the first event, the night values of foF2 remain steadily lower by about 30 percent. Plasma frequencies in the height profile rapidly decrease, increase and decrease in day one, two and three after the event, respectively similarly to the foF2 values (right panel on the Fig. 4). The superstorm of November 7-8, 2004 triggers the strongest response in the ionosphere out of three events we studied.

MC R: Diurnal pattern of foF2 values after the event is more or less normal. There is no significant change of the foF2 mean values for most or the daytime. Night ionization is reduced as seen in Fig. 5. Strong wavelike oscillations in h'F2 are present during last five days and several short–term significant increases of h'F2 do occur. There are no other significant changes in the plasma frequency profile.

Conclusion

Three solar events from February, March and November 2004 are analyzed.

HSS and MC L cause significant change of all discussed ionospheric parameters. The ionospheric response occurs several hours after the onset of geomagnetic storm and in both cases is manifested by a) decrease of foF2, b) increase in heights of F2 layer, and c) decrease of plasma frequency in the height profile, in comparison to reference days. There is a quick recovery to previous typical values in case of MC L two days after the event.

A weaker ionospheric response was observed in the case of MC R. We detected no significant changes of ionospheric parameters compared to the reference days. Oscillations of foF2 and h'F2 are observed similarly as in cases of HSS and MC L.

Several reasons, or more probably, their combination, can be considered to explain dramatic decrease of the plasma density after HSS and MC L events. According to *Tascione*, [1994], ionization/recombination conditions change due to variation of chemical composition during the ionospheric storm, and thus modify rate coefficients. Change in solar flux entering the Earths atmosphere may be another cause. The uplift of the F2 layer with the plasma outflow upward and in the direction along the magnetic field lines may be another explanation. Due to atmospheric wave passage, we may also observe changes in the shapes and heights of the layers (*Sauli et al.*, [2006]). Even though the Dst indices differ strongly in cases of HSS and MC R, the ionospheric responses are comparable. Although Dst index is widely used, it is not sufficient enough for reasonable prediction or description of the state of the ionosphere.

For better understanding of the ionospheric responses to solar events we are planning to choose more solar events and to involve greater number of ionospheric locations to examine longitudinal and latitudinal dependences.

Color version of present paper is available at `http://www.mff.cuni.cz/wds/contents/wds09.htm`.

Acknowledgments. This work has been done in the frame of cooperation agreement between the AS CR and the BAS.

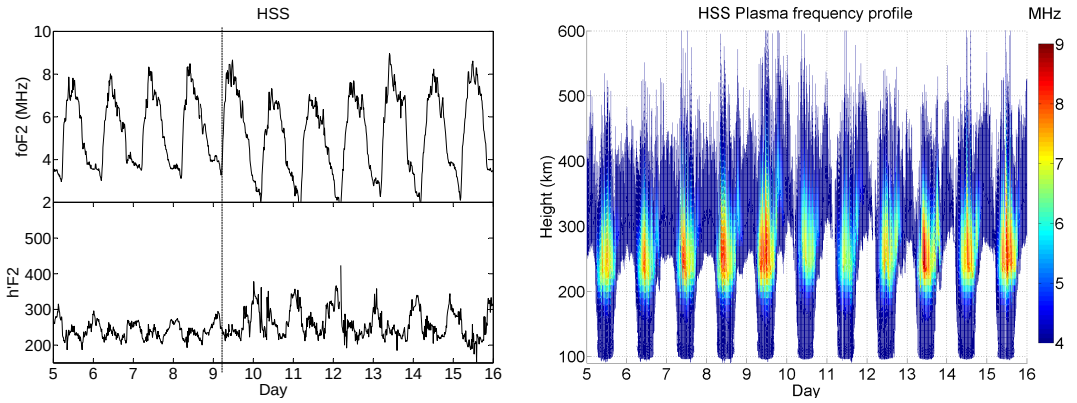

Figure 3. Ionospheric responses in foF2 (top left), h'F2(bottom left) and plasma profile (right) for HSS. Note the reduce in daily and night foF2 and oscillations of h'F2 after the event. Plasma frequency falls in the profile.

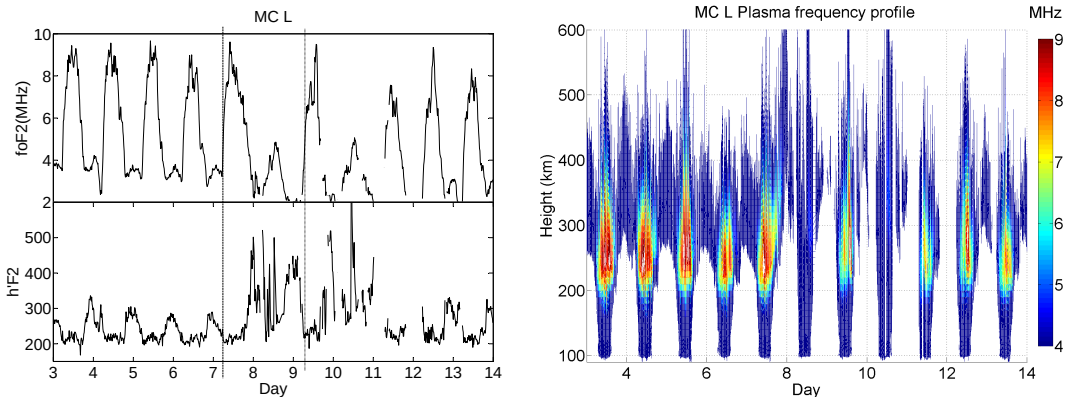

Figure 4. Rapid fall of foF2 one day after MC L is followed by recovery phase and fall again after second event (left upper panel). Strong oscillations in virtual heights are observed (left bottom pannel). Right panel shows changes in plasme frequency profile. The response was so strong that several ionograms are impossible to analyse due to missing reflections.

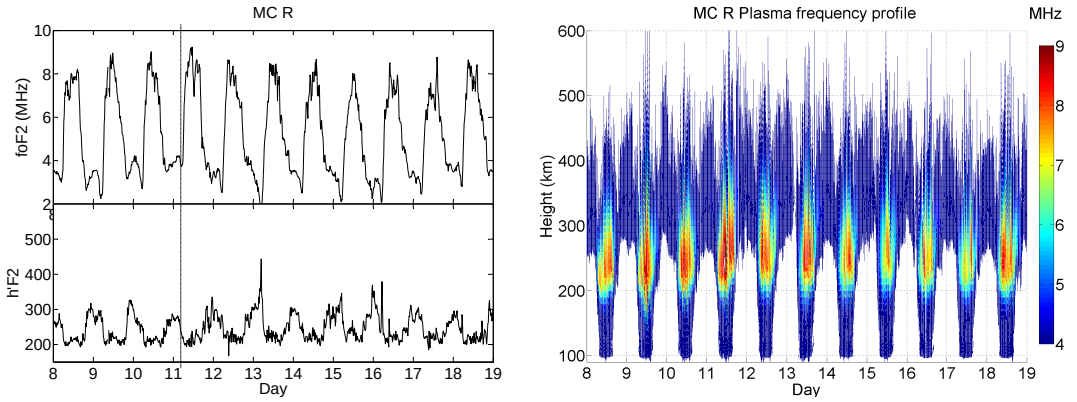

Figure 5. Practically no change in daily values of foF2. Decrease of night foF2 (left upper panel) and oscillations shortly after MC R with several peaks of h'F2 during analysed days (left bottom). No significant change in plasma profile is observed (right panel).

References

Belehaki, A., Cander, L., Zolesi, B., Bremer, J., Juren, C., Stanislawska, I., Dialetis, D., Hatzopoulos, M., Ionospheric specification and forecasting based on observations from European ionosondes participating in DIAS project. *Acta Geophysica*, 55, 3, 398–409, 2007.

Burlaga, L.F., Sittler, E., Mariani, F., Schwenn, R. Magnetic loop behind an interplanetary shock: Voyager, Helios and IMP 8 observations. *Journal of Geophysical Research* 98, 3509, 1981.

Cander, L.R. Ionospheric Ground–based Measurement Networks. *Earth, Moon and Planets* 100, 37-40, 2009.

Davies, K., Ionospheric Radio *Peter Peregrinus Ltd., London*, 1990.

Georgieva, K., Kirov, B., Helicity of magnetic clouds and solar cycle variations of their geoeffectiveness. *Coronal and Stellar Mass Ejections, IAU 226, Cambridge University Press*, 470–472, 2005.

Georgieva, K., Kirov, B., Gavruseva, E., Geoeffectiveness of different solar drivers, and long–term variations of the correlation between sunspot and geomagnetic activity. *Physics and Chemistry of the Earth*, 31, 81–87, 2006.

Hargreaves, J.K., The solar-terrestrial environment. *Cambridge University Press*, 1992.

Huang, X and Reinisch, B. W., Vertical electron density profiles from the digisonde network. *Advances in Space Research*, 18(6), 121–129, 1996.

Mikhailov, A.V., Mikhailov, V.V., Skoblin, M.G., Monthly median foF2 and M(3000)F2 ionospheric model over Europe. *Annali di Geofisica*, 4, 791–805, 1996.

Mosna, Z., Sauli, P., Santolik, O., Analysis of critical frequencies in the ionosphere. *WDS'08 Proceedings of Contributed Papers, Part II*, MATFYZPRESS, 2008.

Reinisch, B.W., Huang X., Galkin I.A., Paznukhov V. and Kozlov A., Recent advances in real–time analysis of ionograms and ionosond drift measurements with digisondes. *Journal of Atmospheric and Sollar–Terr. Physics*, 67, 1054–1062, 2005.

Richardson, I. G., Cliver, E. W., Cane, H. V., Long–term trends in interplanetary magnetic field strength and solar wind structure during the twentieth century. *Journal of Geophysical Research*, 107 (A10), 1304, 2002.

Sauli, P., Mosna, Z., Boska, J., Kouba, D., Lastovicka, J., Altadill, D., Comparison of True–Height Electron Density Profiles Derived by Polan and NHPC Methods. *Studia Geophysica et Geodaetica*, 51, 449–459, 2007.

Sauli P., Abry P., Altadill D., Boska J., Detection of the wave-like structures in the F-region electron density: Two station measurements. *Studia Geophysica et Geodaetica*, 50(1) 131–146, 2006.

Shapley, A.H., Atlas of Ionograms. *World Data Center A, Upper Atmosphere Geophysics*, 1970.

Tascione, T.F., Introduction to the space environment. *Krieger Publishing Company*, 1994.

Zolesi, B., Cander, L.B., De Francheschi, G., Simplified ionospheric regional model. *Radio Science*, 28, 603–612, 1993.